Analyst

RSC Publishing

PAPER

View Article Online
View Journal | View Issue

Cite this: *Analyst*, 2013, **138**, 3264

A highly selective turn-on fluorescent sensor for Cu(II) based on an NSe_2 chelating moiety and its application in living cell imaging†

Cho-Yen Chou, Shi-Rong Liu and Shu-Pao Wu*

Received 6th February 2013
Accepted 28th March 2013

DOI: 10.1039/c3an00286a

www.rsc.org/analyst

In this study, a boron-dipyrromethene (BODIPY)-based fluorescent chemosensor **CBS** was developed for metal ion sensing. It was found that **CBS** containing an NSe_2 moiety exhibited high selectivity for Cu^{2+} detection while **CBS** in the presence of Cu^{2+} displayed significant fluorescence enhancement. However, the metal ions Ag^{+}, Ca^{2+}, Co^{2+}, Cr^{3+}, Fe^{2+}, Fe^{3+}, Hg^{2+}, K^{+}, Mg^{2+}, Mn^{2+}, Ni^{2+}, Pb^{2+}, and Zn^{2+} produced only minor changes in the fluorescence values of the system. The binding constant (K_a) of Cu^{2+} binding to **CBS** was found to be 7.28×10^3 M^{-1}. The binding ratio of **CBS**–Cu^{2+} complexes was determined from the Job plot to be 1 : 1. The maximum fluorescence enhancement caused by Cu^{2+} binding to **CBS** was observed over the pH range 5.0–9.0. Additionally, the methyl thiazolyl tetrazolium (MTT) assay demonstrated the **CBS** to have low cytotoxicity. Confocal fluorescence microscopy imaging using RAW264.7 cells showed that **CBS** could be used as an effective fluorescent probe for detecting Cu^{2+} in living cells.

Introduction

Copper is third in abundance (after iron and zinc) among the essential transition metal ions in the human body and plays an important role in various physiological processes.[1] Many proteins contain copper ions in the catalytic center. Copper ions also catalyze the formation of reactive oxygen species (ROS) that can damage lipids, nucleic acids, and proteins. Several studies have related the cellular toxicity of copper ions to serious diseases including Alzheimer's disease,[2] Indian childhood cirrhosis (ICC),[3] prion disease,[4] and Menkes and Wilson diseases.[5] Due to the extensive use of copper in modern society, copper ions have also become a significant metal pollutant. The limit of copper in drinking water as set by the US Environmental Protection Agency (EPA) is 1.3 ppm (~20 μM).

Several methods have been developed for the detection of copper ions in a sample, such as atomic absorption spectrometry,[6] inductively coupled plasma mass spectroscopy (ICPMS),[7] inductively coupled plasma-atomic emission spectrometry (ICP-AES),[8] and voltammetry.[9] Most of these methods require expensive instruments and cannot be used for on-site detection. As a consequence, more attention is being focused on the development of fluorescent copper sensors that can visualize the cellular distribution of copper ions.[10–28]

A general strategy used in developing metal ion fluorescent sensors is to combine a metal-binding unit with a fluorophore. The presence of target metal ions is indicated by changes in emission intensity or wavelength when the ions interact with the binding units. Because Cu^{2+} is known as a fluorescence quencher, most fluorescent sensors detect Cu^{2+} through a fluorescence quenching process that undergoes an energy or charge transfer mechanism.[13,29] Due to problems with sensitivity, fluorescent sensors that detect metal ions using fluorescence enhancement (turn-on) are easier to be monitored than those using fluorescence quenching (turn-off). This paper reports on a newly designed BODIPY-based fluorescent enhancement sensor for Cu^{2+} based on the photoinduced electron transfer (PET) mechanism. Binding Cu^{2+} to the sensor blocks the PET mechanism and greatly enhances the fluorescence of BODIPY.

In this study, a BODIPY-based fluorescent sensor was designed for metal ion detection. BODIPY, which stands for boron-dipyrromethene, is a fluorescent dye with a high molar absorption coefficient and fluorescence quantum yield.[30] It was used as the signal transduction unit in this study while the NSe_2 moiety behaves as a chelator for the metal ion (Scheme 1). The chemosensor **CBS** (copper binding sensor) exhibits weak fluorescence due to fluorescence quenching by photoinduced electron transfer from the lone pair electrons on the nitrogen atom to the BODIPY. Binding of metal ions to the chemosensor blocks the PET mechanism and results in a great enhancement

Department of Applied Chemistry, National Chiao Tung University, Hsinchu, Taiwan 300, ROC. E-mail: spwu@mail.nctu.edu.tw; Tel: +886-3-5712121 ext. 56506

† Electronic supplementary information (ESI) available: ^1H and ^{13}C NMR spectra of chemosensor **CBS**, ESI mass spectra of the **CBS**–Cu^{2+} complexes and DFT-optimized structure of the **CBS**–Cu^{2+} complexes calculated with the B3LYP/LanL2DZ method are included. See DOI: 10.1039/c3an00286a

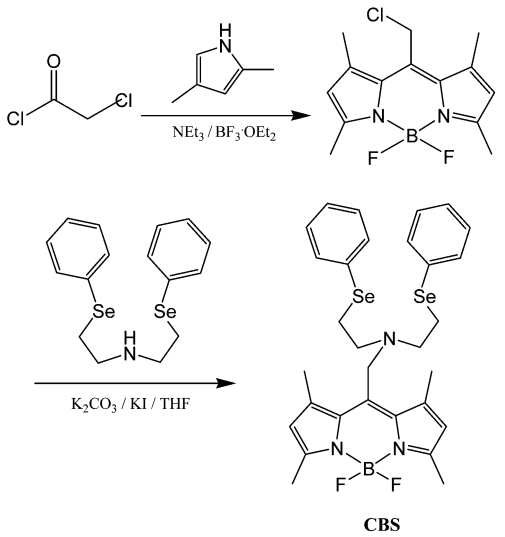

CBS

Scheme 1 Synthesis of chemosensor **CBS**.

in the fluorescence of the BODIPY. The metal ions Ag^{+}, Ca^{2+}, Cr^{3+}, Co^{2+}, Cu^{2+}, Fe^{2+}, Fe^{3+}, Hg^{2+}, K^{+}, Mg^{2+}, Mn^{2+}, Ni^{2+}, Pb^{2+}, and Zn^{2+} were tested for metal ion binding selectivity with **CBS**, but only Cu^{2+} caused a green emission upon binding with **CBS**.

Experimental

Chemicals

$AgClO_4 \cdot \chi H_2O$ and $Pb(ClO_4)_2 \cdot 3H_2O$ were purchased from Acros. $Cr(ClO_4)_3 \cdot 6H_2O$ was purchased from Alfa Aesar. $Ca(ClO_4)_2 \cdot 4H_2O$, $Cd(ClO_4)_2 \cdot \chi H_2O$, $CoCl_2 \cdot 6H_2O$, $Cu(BF_4)_2 \cdot \chi H_2O$, $Cu(ClO_4)_2 \cdot \chi H_2O$, $Fe(BF_4)_2 \cdot 6H_2O$, $FeCl_3 \cdot 6H_2O$, $Hg(ClO_4)_2 \cdot \chi H_2O$, $Mg(ClO_4) \cdot 6H_2O$, $Ni(O_2CCH_3) \cdot 4H_2O$, $Zn(BF_4)_2 \cdot \chi H_2O$ and KBr were purchased from Sigma-Aldrich. $MnSO_4 \cdot H_2O$ was purchased from Riedel-de Haen. For all aqueous solutions, deionized water purified by a Millipore system was used.

Apparatus

UV/Vis spectra were recorded on an Agilent 8453 UV/Vis spectrometer. NMR spectra were obtained on a Bruker DRX-300 NMR and an Agilent Unity INOVA-500 NMR spectrometer. Fluorescence spectra measurements were performed on a Hitachi F-7000 fluorescence spectrophotometer. Fluorescent images were taken on a Leica TCS-SP5-X AOBS Confocal Fluorescence Microscope.

Synthesis of chemosensor CBS

A mixture of 8-[chloromethyl]-4,4-difluoro-1,3,5,7-tetramethyl-4-bora-3*a*,4*a*-diaza-*s*-indacene[31] (1.0 mmol), bis[2-(phenylselenyl)-ethyl]amine[32] (1.0 mmol), potassium iodide (0.25 mmol) and potassium carbonate (1.0 mmol) in 30 mL THF was stirred for 8 h at room temperature under N_2 atmosphere. After filtration, THF was evaporated under reduced pressure. The crude product was purified by column chromatography (hexane : CH_2Cl_2 = 3 : 1) to give compound **CBS** as a red solid. Yield: 226 mg (35%); mp: 125–126 °C. ^{1}H NMR (300 MHz, $CDCl_3$): 7.38 (t, J = 2.7 Hz, 4H), 7.22 (m, 6H), 6.05 (s, 2H), 3.94 (s, 2H), 2.96 (d, J = 3.9 Hz, 4H), 2.89 (d, J = 3.6 Hz, 4H), 2.55 (s, 6H), 2.44 (s, 6H); ^{13}C NMR (125 MHz, $CDCl_3$): 155.2, 141.9, 139.3, 133.0, 132.5, 129.6, 129.1, 126.9, 122.2, 52.6, 49.5, 29.6, 29.1, 25.1, 17.2, 14.6; MS (ESI) found 646.1 $[M + H]^+$; HRMS (ESI) calcd for $C_{29}H_{34}BF_2N_3Se_2$ 646.1223 $[M + H]^+$; found, 646.1252 $[M + H]^+$.

Metal ion binding study by UV-vis and fluorescence spectroscopy

Chemosensor **CBS** (15.0 μM) was added with different metal ions (15.0 μM). All spectra were measured in 1.0 mL acetonitrile–water solution (v/v = 7 : 3, 10 mM Hepes, pH 7.0). The light pathlength of the cuvette was 1.0 cm.

The pH dependence on Cu^{2+} binding in chemosensor 1 studied by fluorescence spectroscopy

Chemosensor **CBS** (15.0 μM) was added with Cu^{2+} (15.0 μM) in 1.0 mL acetonitrile–water solution (v/v = 7 : 3, 10 mM buffer). The buffers were: pH 3–4, CH_3COOH/NaOH; pH 4.5–7.0, MES/NaOH; pH 7.0–10, Hepes.

Determination of the binding stoichiometry and the apparent association constants K_a of Cu(II) binding in chemosensor CBS

The binding stoichiometry of **CBS**–Cu^{2+} complexes was determined by Job plot experiments.[33] The fluorescence intensity at 516 nm was plotted against the molar fraction of **CBS** under a constant total concentration (30.0 μM). The fluorescence approached a maximum intensity when the molar fraction was 0.5. These results indicate that the chemosensor **CBS** forms a 1 : 1 complex with Cu^{2+}. The association constant (K_a) of **CBS**–Cu^{2+} complexes was determined by the consequent equation (1):[34]

$$1/(I - I_0) = 1/\{K_a \times (I_{max} - I_0) \times [Cu^{2+}]\} + 1/(I_{max} - I_0), \quad (1)$$

where I is the fluorescence intensity at 516 nm at any given Cu^{2+} concentration and I_0 is the fluorescence intensity at 516 nm in the absence of Cu^{2+}. The association constant K_a was evaluated graphically by plotting $1/(I - I_0)$ against $1/[Cu^{2+}]$. Typical plots $\{1/(I - I_0)$ *vs.* $1/[Cu^{2+}]\}$ are shown in Fig. 5. Data were linearly fitted according to eqn (1) and the K_a value was obtained from the slope of the line.

Quantum yield determination

The fluorescence quantum yields were determined using rhodamine B as a reference with a known Φ value of 0.49 in EtOH.[35] The sample and the reference were excited at the same wavelength (λ_{ex} = 520 nm), maintaining nearly equal absorbance (0.1) and emission spectra. The quantum yield was calculated according to the following eqn (2):

$$\Phi_S/\Phi_R = (A_S/A_R) \times (Abs_S/Abs_R) \times (\eta_S^2/\eta_R^2), \quad (2)$$

where Φ_S and Φ_R are the fluorescence quantum yields of the sample and the reference, respectively; A_S and A_R are the emission areas of the sample and the reference, respectively; Abs_S and

Abs_R are the corresponding absorbance of the sample and the reference solution at the wavelength of excitation; η_S and η_R are the refractive indices of the sample and the reference, respectively.

Cell culture

RAW264.7 cells were grown in H-DMEM (Dulbecco's Modified Eagle's Medium, high glucose) supplemented with 10% FBS (Fetal Bovine Serum) in an atmosphere of 5% CO_2 at 37 °C.

Cytotoxicity assay

The methyl thiazolyl tetrazolium (MTT) assay was used to measure the cytotoxicity of **CBS** in RAW264.7 cells. RAW264.7 cells were seeded into a 96-well cell-culture plate. Various concentrations (10, 25, 50 μM) of **CBS** were added to the wells. The cells were incubated at 37 °C under 5% CO_2 for 24 h. 10 μL MTT (5 mg mL^{-1}) was added to each well and incubated at 37 °C under 5% CO_2 for 4 h. The MTT solution was removed and yellow precipitates (formazan) observed in plates were dissolved in 200 μL DMSO and 25 μL Sorenson's glycine buffer (0.1 M glycine and 0.1 M NaCl). A Multiskan GO microplate reader was used to measure the absorbance at 570 nm for each well. The viability of cells was calculated according to the following equation:

Cell viability (%) = (mean of absorbance values of the treatment group)/(mean of absorbance values of the control group).

Cell imaging

The cells cultured in DMEM were treated with 10 mM solution of Cu^{2+} (2 μL; final concentration: 20 μM) dissolved in sterilized PBS (pH 7.4) and incubated at 37 °C for 30 min. The treated cells were washed with PBS (2 mL × 3) to remove the remaining metal ions. DMEM (2 mL) was added to the cell culture, which was then treated with a 10 mM solution of chemosensor **CBS** (2 μL; final concentration: 20 μM) dissolved in DMSO. The samples were incubated at 37 °C for 30 min. The culture medium was removed, and the treated cells were washed with PBS (2 mL × 3) before observation. Fluorescence imaging was performed with a Leica TCS-SP5-X AOBS Confocal microscope. The cells were excited with a white light laser at 488 nm, and the emission was collected at 530 ± 10 nm.

Computational methods

Quantum chemical calculations based on density functional theory (DFT) were carried out using a Gaussian 09 program. The ground-state structures of **CBS** and the **CBS**–Cu^{2+} complexes were computed using the density functional theory (DFT) method with the hybrid-generalized gradient approximation (HGGA) functional B3LYP. The 6-31G basis set was assigned to nonmetal elements (C, H, N, B, F, and Se). For the **CBS**–Cu^{2+} complex, the LANL2DZ basis set was used for Cu^{2+}, whereas the 6-31G basis set was used for other atoms.

Results and discussion

Synthesis of CBS

The synthesis of the fluorescent probe, **CBS**, is outlined in Scheme 1. **CBS** was obtained by the reaction of 8-[chloromethyl]-4,4-difluoro-1,3,5,7-tetramethyl-4-bora-3*a*,4*a*-diaza-*s*-indacene and bis[2-(phenylselenyl)ethyl]amine under weak base conditions in THF (tetrahydrofuran). **CBS** exhibits weak fluorescence ($\Phi = 0.006$) compared to BODIPY.[30] This is due to fluorescence quenching by photoinduced electron transfer from the lone pair electrons on the nitrogen atom to the BODIPY.

Cation-sensing properties

The sensing ability of **CBS** was tested by mixing it with the metal ions Ag^{+}, Ca^{2+}, Cr^{3+}, Co^{2+}, Cu^{2+}, Fe^{2+}, Fe^{3+}, Hg^{2+}, K^{+}, Mg^{2+}, Mn^{2+}, Ni^{2+}, Pb^{2+}, and Zn^{2+}. Cu^{2+} was the only ion that caused a green emission from **CBS** (Fig. 1). During Cu^{2+} titration with **CBS**, a new emission band centered at 516 nm was formed (Fig. 2). After adding 1.0 equivalent of Cu^{2+}, the emission intensity reached a maximum. The quantum yield of the emission band was 0.11, which is 18-fold that of **CBS** at 0.006. These observations indicate that Cu^{2+} is the only metal ion that readily binds with **CBS**, causing significant fluorescence enhancement and permitting highly selective detection of Cu^{2+}.

To study the influence of other metal ions on Cu^{2+} binding with **CBS**, competitive experiments were performed with other metal ions (15.0 μM) in the presence of Cu^{2+} (15.0 μM) (Fig. 3). It was found that fluorescence enhancement caused by the mixture of Cu^{2+} with most metal ions was similar to that caused by Cu^{2+} alone. Smaller fluorescence enhancement was observed

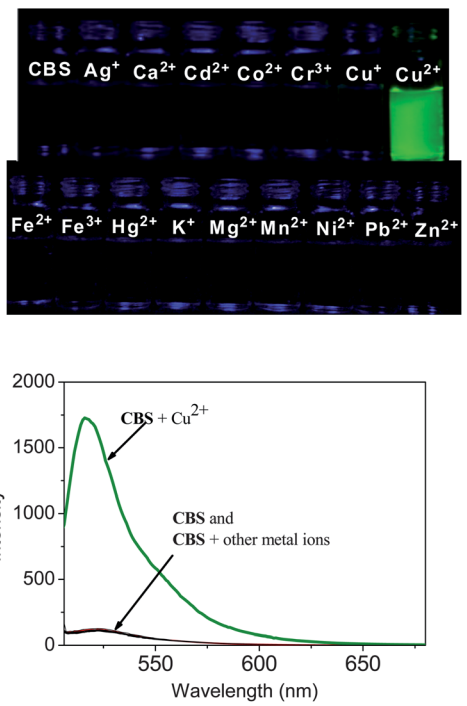

Fig. 1 Fluorescence change of **CBS** (15.0 μM) upon addition of various metal ions (15.0 μM) in acetonitrile–water (v/v = 7 : 3, 10 mM HEPES, pH 7.0) solutions.

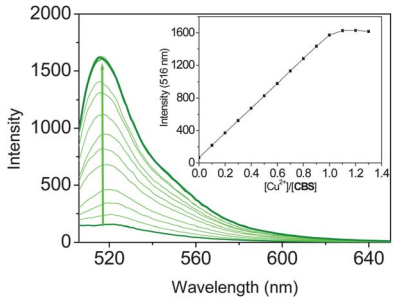

Fig. 2 Fluorescence response of **CBS** (15.0 μM) to various equivalents of Cu^{2+} in acetonitrile–water (v/v = 7 : 3, 10 mM HEPES, pH 7.0) solutions. The excitation wavelength was 500 nm.

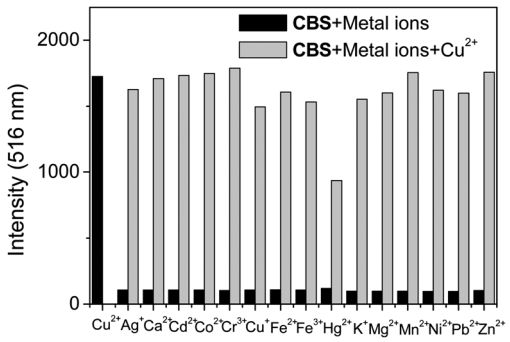

Fig. 3 Fluorescence response of the chemosensor **CBS** (15.0 μM) to Cu^{2+} (15.0 μM) or 15.0 μM of other metal ions (black bars) and to the mixture of other metal ions (15.0 μM) with 15.0 μM of Cu^{2+} (gray bars) in acetonitrile–water (v/v = 7 : 3, 10 mM HEPES, pH 7.0) solutions.

only when Cu^{2+} was mixed with Hg^{2+}, which indicates that Hg^{2+} competes with Cu^{2+} for binding with **CBS**. None of the other metal ions were found to interfere with the binding of **CBS** with Cu^{2+}.

In order to understand the binding stoichiometry of **CBS**–Cu^{2+} complexes, Job plot experiments were carried out. In Fig. 4, the emission intensity at 516 nm is plotted against the molar fraction of **CBS** under a constant total concentration (30.0 μM). Maximum emission intensity was reached when the molar fraction was 0.50. Results indicated a 1 : 1 ratio for

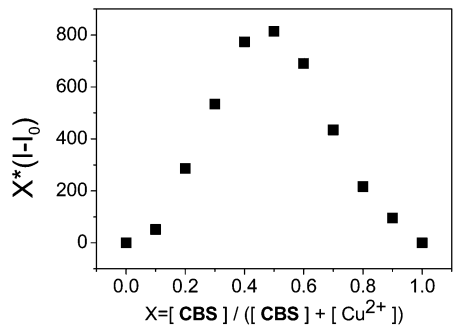

Fig. 4 Job plot of the **CBS**–Cu^{2+} complexes in an acetonitrile–water (v/v = 7 : 3, 10 mM HEPES, pH 7.0) solution. The total concentration of **CBS** and Cu^{2+} was 30.0 μM. The monitored wavelength was 516 nm.

CBS–Cu^{2+} complexes, in which one Cu^{2+} ion was bound to one **CBS**. The formation of a 1 : 1 **CBS**–Cu^{2+} complex was confirmed by ESI-MS; the peak at m/z = 707.8 indicated a 1 : 1 stoichiometry for the **CBS**–Cu^{2+} complex (see Fig. S4 in the ESI†). The association constant K_a was evaluated graphically by plotting $1/(I - I_0)$ against $1/[Cu^{2+}]$ (Fig. 5). The data were linearly fit and the K_a value was obtained from the slope and intercept of the line. The association constant (K_a) of Cu^{2+} binding in **CBS** was found to be 7.28×10^3 M^{-1}. The detection limit of **CBS** as a fluorescent sensor for the analysis of Cu^{2+} was determined from the plot of fluorescence intensity as a function of the concentration of Cu^{2+} (see Fig. S5 in the ESI†). **CBS** was found to have a detection limit of 0.87 μM, which means it is able to detect Cu^{2+} concentrations in the micro-molar range.

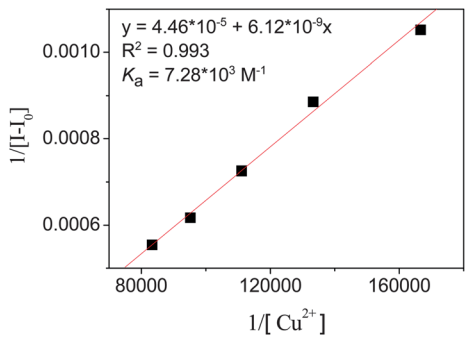

Fig. 5 Benesi–Hildebrand plot of **CBS** with Cu^{2+} in CH_3CN/H_2O (v/v = 7 : 3, 10 mM HEPES, pH 7.0). The excitation wavelength was 500 nm and the observed wavelength was 516 nm. The binding constant was 7.28×10^3 M^{-1} for Cu^{2+} binding in **CBS**.

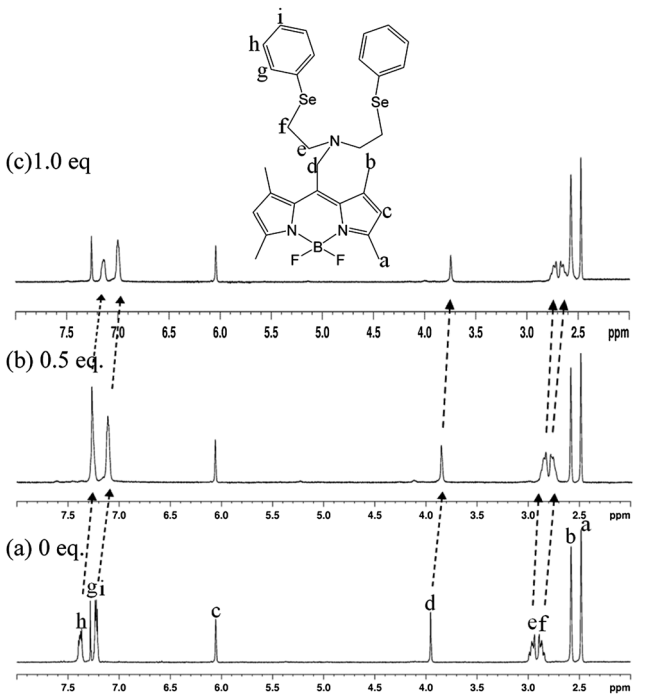

Fig. 6 ^1H NMR 300 MHz spectra of **CBS** (10.0 mM) upon titration with various equivalents of Cu^{2+} in $CDCl_3$/DMSO-d_6 (v/v = 9 : 1).

To gain a clearer understanding of the structure of **CBS**–Cu^{2+} complexes, ^{1}H NMR spectroscopy was employed (Fig. 6). Cu^{2+} is a paramagnetic ion and can therefore affect the proton signals that are close to the Cu^{2+} binding site. The ^{1}H NMR spectra of **CBS** recorded with increasing amounts of Cu^{2+} show that the proton (H_d, H_e, and H_f) signals shifted upfield as more and more Cu^{2+} was added. This indicates that Cu^{2+} binds to **CBS** mainly through the nitrogen atom and two selenium atoms. The proton signals (H_g, H_h, and H_i) in the phenyl ring also showed upfield shifts upon the addition of Cu^{2+}. This indicated that Cu^{2+} binds to the selenium atoms that are attached to the phenyl ring and Cu^{2+} binding affects the ring current at the phenyl ring.

To elucidate the structures of **CBS** and **CBS**–Cu^{2+} complexes, density functional theory (DFT) calculations were undertaken using the Gaussian 09 software package. Chemosensor **CBS** and **CBS**–Cu^{2+} complexes were subjected to energy optimization by using B3LYP/6-31G and B3LYP/LANL2DZ, respectively. The global minima structures for **CBS** and **CBS**–Cu^{2+} complexes are shown in Fig. 7. The distances of Cu^{2+} from the two selenium atoms were 2.47 Å and 2.41 Å, and from the nitrogen atom was 2.11 Å.

Density functional theory (DFT) calculation was also applied to determine the detecting mechanism of **CBS** for Cu^{2+}. As shown in Scheme 2, the highest occupied molecular orbital (HOMO) of the bis[2-(phenylselenyl)ethyl]amine moiety (electron donor) matches that of the fluorophore BODIPY (electron acceptor); the HOMO energy level (−5.18 eV) of the bis[2-(phenylselenyl)ethyl]amine moiety is higher than that of the fluorophore BODIPY (−5.73 eV). Consequently, when the BODIPY moiety is excited by light, the intramolecular electron transfer from the bis[2-(phenylselenyl)ethyl]amine moiety to the BODIPY moiety is energetically allowed. Hence, the fluorescence of the BODIPY moiety is quenched through a PET process ($\Phi < 0.01$). In contrast, upon the complexation of **CBS** by Cu^{2+}, the HOMO energy level of the bis[2-(phenylselenyl)ethyl]amine

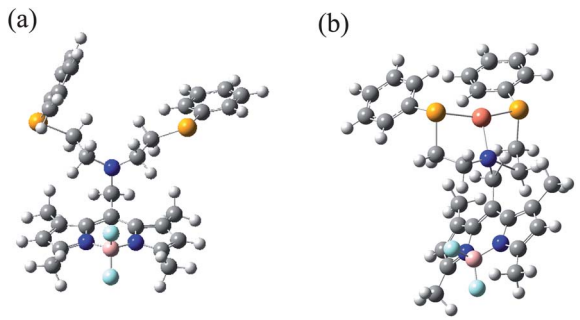

Fig. 7 DFT-optimized structures of (a) **CBS** and (b) **CBS**–Cu^{2+} complexes. Blue atom, N; red atom, Cu; yellow atom, Se.

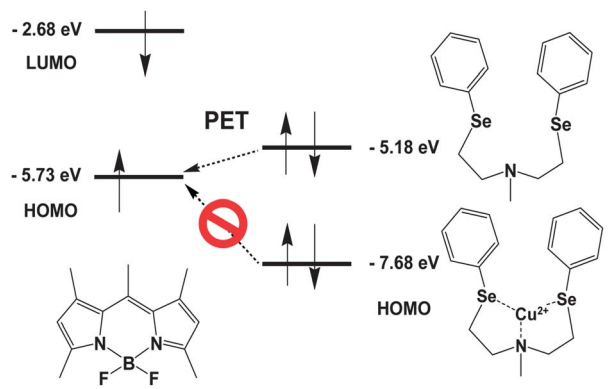

Scheme 2 Energy diagram for the reaction of **CBS** with Cu^{2+}.

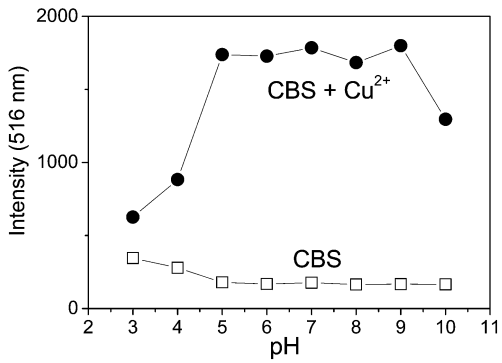

Fig. 8 Fluorescence response (516 nm) of free chemosensor **CBS** (15.0 μM) and after addition of Cu^{2+} (15.0 μM) in CH_3CN/H_2O (v/v = 7 : 3, 10 mM buffer) solution as a function of different pH values. The excitation wavelength was 500 nm.

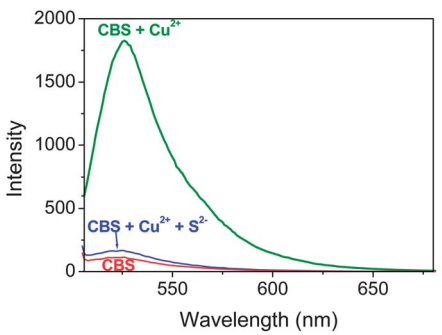

Fig. 9 Reversibility of the interaction between **CBS** and Cu^{2+} by the introduction of S^{2-} to the system.

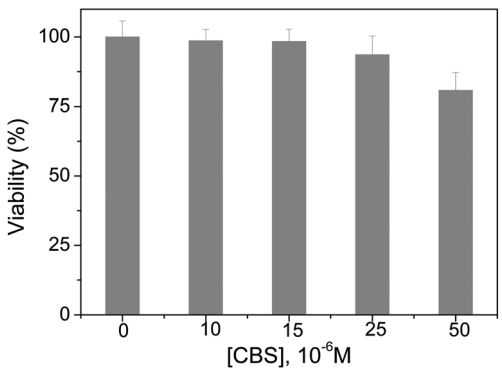

Fig. 10 Cell viability values (%) estimated by an MTT assay *versus* incubation concentrations of **CBS**. RAW264.7 cells were cultured in the presence of **CBS** (0–50 μM) at 37 °C for 24 h.

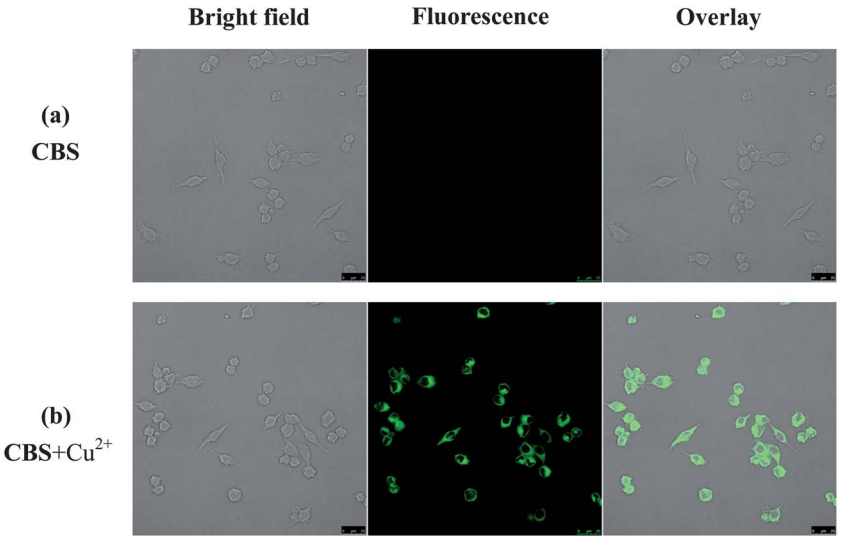

Fig. 11 Fluorescence images of RAW264.7 cells treated with **CBS** and Cu^{2+}. (Left) Bright field image; (middle) fluorescence image; (right) merged image. The scale bar is 25 μm.

moiety (−7.68 eV) is lower than that of the BODIPY unit; therefore, the PET process is restricted and the fluorescence of BODIPY is restored.

We performed pH titration of **CBS** to investigate a suitable pH range for Cu^{2+} sensing. As depicted in Fig. 8, the emission intensities of metal-free **CBS** were very low. After mixing the chemosensor **CBS** with Cu^{2+}, the emission intensity at 516 nm suddenly increased at pH 5.0 and reached a maximum in the pH range of 5.0 to 9.0. The emission intensity decreases at pH > 9.0. This indicates poor stability of the **CBS**–Cu^{2+} complexes at high pH. For pH < 5, the emission intensity is very low due to the protonation of the amine group, which prevents the formation of **CBS**–Cu^{2+} complexes.

For a chemosensor to be extensively used in the detection of specific targets, the reversibility is an important issue. To explore whether the binding process of the chemosensor **CBS** with Cu^{2+} was reversible, an excess amount of S^{2-} was added into the solution of the chemosensor **CBS** with Cu^{2+}. In Fig. 9, the emission peak at 516 nm decreases significantly after the addition of S^{2-}. When Cu^{2+} was added to the system, the fluorescence of **CBS** was enhanced again. This observation indicated the reversible binding character of the chemosensor **CBS** with Cu^{2+}.

Living cell imaging

The potential of **CBS** for imaging Cu^{2+} in living cells was investigated next. First, an MTT assay with a RAW264.7 cell line was used to determine the cytotoxicity of **CBS**. In Fig. 10, the cellular viability was estimated to be greater than 80% after 24 h, which indicates that **CBS** (<50 μM) has low cytotoxicity. Furthermore, the images of cells were obtained using a confocal fluorescence microscope. When RAW264.7 cells were incubated with **CBS** (10 μM), no fluorescence was observed (Fig. 11a). After the treatment with Cu^{2+}, bright green fluorescence was observed in the RAW264.7 cells (Fig. 11b). An overlay of fluorescence and bright-field images shows that the fluorescence signals are localized in the intracellular area, indicating a subcellular distribution of Cu^{2+} and good cell-membrane permeability of **CBS**.

Conclusion

In conclusion, we developed a BODIPY-based fluorescent chemosensor for Cu^{2+} sensing. We observed significant fluorescence enhancement with **CBS** in the presence of Cu^{2+}. However, adding Ag^{+}, Ca^{2+}, Cr^{3+}, Co^{2+}, Fe^{2+}, Fe^{3+}, Hg^{2+}, K^{+}, Mg^{2+}, Mn^{2+}, Ni^{2+}, Pb^{2+}, or Zn^{2+} to the chemosensor solution caused only minimal changes in fluorescence emission. The optimal pH range for Cu^{2+} detection by **CBS** is 5.0–9.0. In addition, the chemosensor **CBS** has low cytotoxicity and therefore can be applied for detecting Cu^{2+} in living cells.

Acknowledgements

We gratefully acknowledge the financial support from the National Science Council (ROC) and National Chiao Tung University.

References

1 J. A. Cowan, *Inorganic Biochemistry: An Introduction*, Wiley-VCH, New York, 1997, pp. 133–134.
2 K. J. Barnham, C. L. Masters and A. I. Bush, *Nat. Rev. Drug Discovery*, 2004, **3**, 205–214.
3 S. H. Hahn, M. S. Tanner, D. M. Danke and W. A. Gahl, *Biochem. Mol. Med.*, 1995, **54**, 142–145.
4 D. R. Brown, *Brain Res. Bull.*, 2001, **55**, 165–173.
5 D. J. Waggoner, T. B. Bartnikas and J. D. Gitlin, *Neurobiol. Dis.*, 1999, **6**, 221–230.
6 A. P. S. Gonzales, M. A. Firmino, C. S. Nomura, F. R. P. Rocha, P. V. Oliveira and I. Gaubeur, *Anal. Chim. Acta*, 2009, **636**, 198–204.

7 J. S. Becker, A. Matusch, C. Depboylu, J. Dobrowolska and M. V. Zoriy, *Anal. Chem.*, 2007, **79**, 3208–3216.
8 Y. Liu, P. Liang and L. Guo, *Talanta*, 2005, **68**, 25–30.
9 P. Pathirathna, Y. Yang, K. Forzley, S. P. McElmurry and P. Hashemi, *Anal. Chem.*, 2012, **84**, 6298–6302.
10 X. Zhang, Y. Shiraishi and T. Hirai, *Org. Lett.*, 2007, **9**, 5039–5042.
11 G. Li, Z. Xu, C. Chen and Z. Huang, *Chem. Commun.*, 2008, 1774–1776.
12 S. Wu and S. Liu, *Sens. Actuators, B*, 2009, **141**, 187–191.
13 H. S. Jung, P. S. Kwon, J. W. Lee, J. Kim, C. S. Hong, J. W. Kim, S. Yan, J. Y. Lee, J. W. Lee, T. Joo and S. Kim, *J. Am. Chem. Soc.*, 2009, **131**, 2008–2012.
14 H. S. Jung, M. Park, D. Y. Han, E. Kim, C. Lee, S. Ham and J. S. Kim, *Org. Lett.*, 2009, **11**, 3378–3381.
15 H. Y. Lee, H. Son, J. M. Lim, J. Oh, D. Kang, W. S. Han and J. H. Jung, *Analyst*, 2010, **135**, 2022–2027.
16 S. Goswami, D. Sen and N. K. Das, *Org. Lett.*, 2010, **12**, 856–859.
17 S. Wu, T. Wang and S. Liu, *Tetrahedron*, 2010, **66**, 9655–9658.
18 D. Maity and T. Govindaraju, *Chem.–Eur. J.*, 2011, **17**, 1410–1414.
19 Y. Li, X. Zhang, B. Zhu, J. Xue, Z. Zhu and W. Tan, *Analyst*, 2011, **136**, 1124–1128.
20 M. P. Algi, Z. Oztas and F. Algi, *Chem. Commun.*, 2012, **48**, 10219–10221.
21 J. Jo, H. Y. Lee, W. Liu, A. Olasz, C. Chen and D. Lee, *J. Am. Chem. Soc.*, 2012, **134**, 16000–16007.
22 K. Li, N. Li, X. Chen and A. Tong, *Anal. Chim. Acta*, 2012, **712**, 115–119.
23 Z. Liu, C. Zhang, X. Wang, W. He and Z. Guo, *Org. Lett.*, 2012, **14**, 4378–4381.
24 J. Fan, X. Liu, M. Hu, H. Zhu, F. Song and X. Peng, *Anal. Chim. Acta*, 2012, **735**, 107–113.
25 J. Liu, L. Lin, X. Wang, S. Lin, W. Cai, L. Zhang and Z. Zheng, *Analyst*, 2012, **137**, 2637–2642.
26 A. Salinas-Castillo, M. Ariza-Avidad, C. Pritz, M. Camprubí-Robles, B. Fernández, M. J. Ruedas-Rama, A. M. Fernández, A. Lapresta-Fernández, F. Santoyo-Gonzalez, A. Schrott-Fischerb and L. F. Capitan-Vallveya, *Chem. Commun.*, 2013, **49**, 1103–1105.
27 C. Kar, M. D. Adhikari, A. Ramesh and G. Das, *Inorg. Chem.*, 2013, **52**, 743–752.
28 W. Wang, Q. Wen, Y. Zhang, X. Fei, Y. Li, Q. Yang and X. Xu, *Dalton Trans.*, 2013, **42**, 1827–1833.
29 M. Pamuk and F. Algi, *Tetrahedron Lett.*, 2012, **53**, 7117–7120.
30 (*a*) A. Loudet and K. Burgess, *Chem. Rev.*, 2007, **107**, 4891–4932; (*b*) G. Ulrich, R. Ziessel and A. Harriman, *Angew. Chem., Int. Ed.*, 2008, **47**, 1184–1201; (*c*) M. Benstead, G. H. Mehl and R. W. Boyle, *Tetrahedron*, 2011, **67**, 3573–3601.
31 S. Huang, S. He, Y. Lu, F. Wei, X. Zeng and L. Zhao, *Chem. Commun.*, 2011, **47**, 2408–2410.
32 M. Tian, X. Peng, F. Feng, S. Meng, J. Fan and S. Sun, *Dyes Pigm.*, 2009, **81**, 58–62.
33 A. Senthilvelan, I. Ho, K. Chang, G. Lee, Y. Liu and W. Chung, *Chem.–Eur. J.*, 2009, **15**, 6152–6160.
34 H. A. Benesi and J. H. Hildebrand, *J. Am. Chem. Soc.*, 1949, **71**, 2703–2707.
35 K. G. Casey and E. L. Quitevis, *J. Phys. Chem.*, 1988, **92**, 6590–6594.

